Nonlin. Processes Geophys., 18, 381–388, 2011
www.nonlin-processes-geophys.net/18/381/2011/
doi:10.5194/npg-18-381-2011

Nonlinear Processes in Geophysics

A semi-phenomenological approach to explain the event-size distribution of the Drossel-Schwabl forest-fire model

S. Hergarten and R. Krenn

Institut für Erdwissenschaften, Karl-Franzens-Universität Graz, Heinrichstraße 26, 8010 Graz, Austria

Received: 17 March 2011 – Revised: 15 June 2011 – Accepted: 19 June 2011 – Published: 21 June 2011

Abstract. We present a novel approach to explain the complex scaling behavior of the Drossel-Schwabl forest-fire model in two dimensions. Clusters of trees are characterized by their size and perimeter only, whereas spatial correlations are neglected. Coalescence of clusters is restricted to clusters of similar sizes. Our approach derives the value of the scaling exponent τ of the event size distribution directly from the scaling of the accessible perimeter of percolation clusters. We obtain $\tau = 1.19$ in the limit of infinite growth rate, in perfect agreement with numerical results. Furthermore, our approach predicts the unusual transition from a power law to an exponential decay even quantitatively, while the exponential decay at large event sizes itself is reproduced only qualitatively.

1 Introduction

The Drossel-Schwabl forest-fire model (DS-FFM in the following) (Drossel and Schwabl, 1992) is one of the three most widespread models in the context of self-organized criticality (SOC) (Bak et al., 1987; Bak, 1996; Jensen, 1998). Although it is nearly 20 yr old, many questions concerning its characteristics remain to be answered. Analytical theories are still lacking; almost the entire knowledge about the DS-FFM stems from numerical simulations.

The DS-FFM is a stochastic cellular automaton model mostly considered on a two-dimensional square lattice with $L \times L$ sites and periodic boundary conditions. Each site can be either empty or occupied by a tree. In each time step, θ attempts are made to plant new trees on randomly selected sites. Empty sites turn into the state occupied, while already occupied sites keep their state. Then, one site is randomly chosen. If this site is occupied, the entire cluster of occupied sites connected to it by nearest-neighbor relations burns down.

After a transient phase, the system reaches a quasi-steady state that seems to be characterized by power-law event-size distributions in the limit of large growth rates θ: The statistical distribution related to the event size s (measured in terms of the number of burnt trees) decreases like $s^{-\tau}$, where τ is typically denoted scaling exponent. Fig. 1 gives the frequency density $u(s)$ of the fires (i.e., the number of fires per spark) for different growth rates θ. These results suggest that the scaling exponent τ converges towards 1.19 for $\theta \to \infty$, in perfect agreement with the presumably most reliable earlier results of Grassberger (2002) and Pruessner and Jensen (2002).

Although its applicability to real wildfires has been shown (Malamud et al., 1998; Zinck and Grimm, 2008; Krenn and Hergarten, 2009) and much effort has been spent to quantify the behavior of the DS-FFM numerically (Moßner et al., 1992; Grassberger, 1993; Christensen et al., 1993; Henley, 1993; Clar et al., 1994; Honecker and Peschel, 1997; Pastor-Satorras and Vespignani, 2000; Grassberger, 2002; Pruessner and Jensen, 2002; Schenk et al., 2002), there is still no consistent explanation for major parts of its dynamics. This applies in particular to the transition from the power-law regime to an exponential decay which is more complicated than in other models of SOC such as the Bak-Tang-Wiesenfeld sandpile model (Bak et al., 1987) or the Olami-Feder-Christensen earthquake model (Olami et al., 1992). As illustrated in Fig. 1, the event-size distribution first increases relatively to the power law and then decays rapidly. This unusual bump in the distribution even makes it difficult to determine the scaling exponent τ of the power-law regime numerically.

Correspondence to: S. Hergarten
(stefan.hergarten@uni-graz.at)

Published by Copernicus Publications on behalf of the European Geosciences Union and the American Geophysical Union.

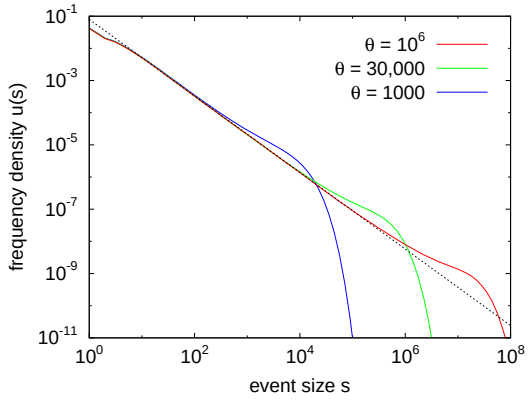

Fig. 1. Frequency density of the fires in the DS-FFM for different growth rates θ. The dashed line corresponds to a power law with an exponent $\tau = 1.19$.

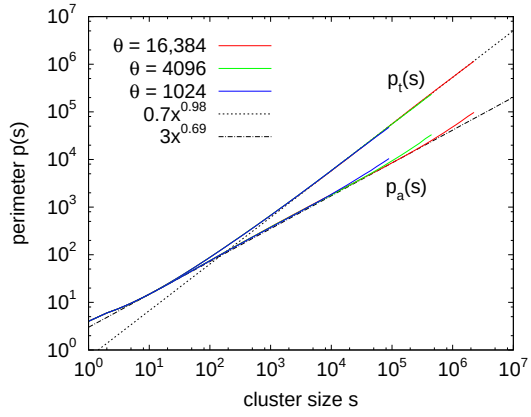

Fig. 2. Total and accessible perimeter of the clusters in the DS-FFM measured at different growth rates θ.

2 A simple approach to derive the scaling exponent

We now derive a semi-phenomenological approach to explain this behavior where clusters are characterized only by their size without regard to spatial correlations between clusters. In its spirit, this idea is similar to the hierarchical clustering idea of Gabrielov et al. (1999). Under some extreme simplifications, they obtained a scaling exponent $\tau = 1$ which is significantly lower than that of the DS-FFM.

Let $N(s)$ be the number of clusters of size s on a lattice of total size $A = L^2$. Like in the DS-FFM, the dynamics of our model is governed by formation of new clusters, growth of existing clusters, coalescence of clusters, and annihilation of clusters by burning.

The probability that a given cluster of size s is burnt down by an ignition event is simply $\frac{s}{A}$, so each ignition event changes the number of clusters of size s by

$$\delta N_b(s) = -N(s)\frac{s}{A} = -u(s) \tag{1}$$

with $u(s) = \frac{N(s)s}{A}$ in the mean. Obviously, $u(s)$ is the mean number of fires of size s per ignition event, i.e., the frequency density of the event-size distribution.

After each ignition event, θ attempts are made to plant new trees. An existing cluster of size s grows if a new tree is planted on its total perimeter $p_t(s)$. Since clusters are not dense in general, the total perimeter consists of both external and internal empty nearest-neighbor sites. As Fig. 2 demonstrates, the total perimeter $p_t(s)$ is almost proportional to the cluster size for large clusters. Our numerical data suggest the relationship $p_t(s) = 0.7s^{0.98}$, but for simplicity we assume

$$p_t(s) = fs \tag{2}$$

with $f = 0.7$ in the following. The same relationship was originally derived for site percolation clusters at and above the percolation threshold by Kunz and Souillard (1978), and our results show that it is valid for clusters in the DS-FFM, too. Planting θ new trees lets $\theta N(s)\frac{p_t(s)}{A}$ clusters grow from size s to $s+1$. Therefore, the number of clusters of size s changes by

$$\begin{aligned}\delta N_g(s) &= \theta N(s-1)\frac{p_t(s-1)}{A} - \theta N(s)\frac{p_t(s)}{A} \\ &= -\theta f\,(u(s) - u(s-1)).\end{aligned} \tag{3}$$

At this point one may argue that several trees may grow at the perimeter of a single cluster in case of high growth rates or large clusters. According to Eq. (3), k clusters would increase their size by one instead of one cluster by k. However, both modes of growth act almost in the same way on the size distribution, which will become obvious when we switch from the discrete representation to a differential equation (Eq. 11).

Coalescence of clusters takes place if a tree grows at a site which belongs to the perimeter of two or more clusters. In analogy to the widespread approach using Smoluchowski's coagulation equation with a suitable kernel, we neglect coalescence events involving more than two clusters. In contrast to growth, not all sites of a cluster's total perimeter are available for coalescence. Sites belonging to the internal part of the perimeter can only contribute to coalescence with clusters located like islands in a hole of the original cluster. Thus, coalescence via internal perimeter sites is in principle only possible between clusters of strongly different sizes. As discussed later, this mechanism is not very efficient.

We therefore assume that coalescence does not depend on the total perimeter of clusters, but on the so-called accessible perimeter $p_a(s)$. It consists of those perimeter sites which can be reached, in principle, by a random walker coming

from infinity (Grossman and Aharony, 1986). The accessible perimeter was recently used in a modified forest-fire model to mimic ignition by human impact (Krenn and Hergarten, 2009). Numerical results on the total and the accessible perimeter are shown in Fig. 2. Due to the significantly higher numerical effort for evaluating perimeters, growth rates are smaller than those used to examine the event-size distributions. For geometric reasons, total and accessible perimeters must be the same for all clusters with $s \le 6$, while a significant deviation $p_a(s) < p_t(s)$ becomes visible for $s \ge 20$. Figure 2 reveals that the accessible perimeter scales like

$$p_a(s) = g s^h \tag{4}$$

with $g = 3$ and $h = 0.69$ for intermediate cluster sizes. As discussed by Krenn and Hergarten (2009), this behavior is almost identical to that obtained for site percolation clusters by combining numerical results on the fractal dimension of the accessible perimeter (Grossman and Aharony, 1986) with theoretical arguments. The θ-dependent deviation from the power law at large cluster sizes will be discussed in the next section.

The probability that a given pair of clusters of sizes s_1 and s_2 coalesce when a new tree is planted amounts to $\frac{p_a(s_1)}{A}\frac{p_a(s_2)}{A}$. In principle, clusters of any sizes can coalesce, but the process is most efficient in generating large clusters if both clusters are of similar sizes. In this case, the largest new cluster is about twice as large as the original clusters. In contrast, coalescence of a large cluster with a small cluster increases the size of the large cluster only gradually. We therefore only consider the case that one size is not larger than twice the other size, i.e. that two clusters with sizes in the interval $[\frac{1}{2}\sqrt{2}s, \sqrt{2}s]$ turn into one cluster with a size between $\sqrt{2}s$ and $2\sqrt{2}s$. The number of clusters in this interval is approximately

$$\hat{N}(s) = \sqrt{\frac{1}{2}} s N(s). \tag{5}$$

It is easily verified that Eq. (5) is exact if $N(s)$ is constant or $N(s) \propto s^{-2}$. However, the cluster numbers in the DS-FFM follow the relationship $N(s) \propto s^{-\tau-1}$ where τ is the scaling exponent of the fire-size distribution. In this case, Eq. (5) changes into $\hat{N}(s) = \frac{\sqrt{2}^\tau - \sqrt{2}^{-\tau}}{\tau} s N(s)$, but it can easily be checked that the difference towards Eq. (5) is less than 2 % for $0 \le \tau \le 1.4$.

Using Eq. (5), the number of pairs in the interval $[\frac{1}{2}\sqrt{2}s, \sqrt{2}s]$ is $\frac{1}{2}\left(\hat{N}(s)\right)^2 = \frac{1}{2}\left(\sqrt{\frac{1}{2}} s N(s)\right)^2$, so that the number of coalescence events is roughly $\theta\frac{1}{2}\left(\sqrt{\frac{1}{2}} s N(s)\right)^2 \left(\frac{p_a(s)}{A}\right)^2$.

Thus, the number of clusters in the interval $[\frac{1}{2}\sqrt{2}s, \sqrt{2}s]$ changes by

$$\sqrt{\frac{1}{2}} s \delta N_c(s) = \theta\frac{1}{2}\left(\sqrt{\frac{1}{2}}\frac{s}{2} N\left(\frac{s}{2}\right)\right)^2 \left(\frac{p_a(\frac{s}{2})}{A}\right)^2 - 2\theta\frac{1}{2}\left(\sqrt{\frac{1}{2}} s N(s)\right)^2 \left(\frac{p_a(s)}{A}\right)^2, \tag{6}$$

where the factor 2 in the second line states that two clusters vanish in a single coalescence event. This can be rewritten in the form

$$\delta N_c(s) = -\frac{\theta}{\sqrt{2}s^2}\left(s p_a(s)^2 u(s)^2 - \frac{s}{2} p_a\left(\frac{s}{2}\right)^2 u\left(\frac{s}{2}\right)^2\right). \tag{7}$$

Strictly speaking, this approach neglects the contribution of the connecting tree itself on the size of the resulting cluster. But in return, we did not subtract the overlap of accessible perimeters when computing growth (Eq. 3), so that this (anyhow small) effect is compensated.

As soon as the system has reached its quasi-steady state, coalescence, growth, formation of new clusters, and burning must be in equilibrium:

$$\delta N_c(s) + \delta N_g(s) + \delta N_f(s) + \delta N_b(s) = 0, \tag{8}$$

where the formation of new clusters $\delta N_f(s)$ vanishes for $s > 1$. Inserting Eqs. (1), (3), and (7) leads to the equilibrium condition

$$\frac{1}{\sqrt{2}s^2}\left(s p_a(s)^2 u(s)^2 - \frac{s}{2} p_a\left(\frac{s}{2}\right)^2 u\left(\frac{s}{2}\right)^2\right) + f\left(u(s) - u(s-1)\right) + \frac{u(s)}{\theta} = 0 \tag{9}$$

for $s > 1$. Alternatively, Eq. (9) can be transformed into a differential equation. Since the term in the first parentheses can be seen as a discrete representation of the differential operator

$$\frac{d}{d\log_2 s} = \log 2 \frac{d}{d\log s} = s \log 2 \frac{d}{ds} \tag{10}$$

and $\log 2 \approx \sqrt{\frac{1}{2}}$, we arrive at

$$\frac{1}{2s}\frac{d}{ds}\left(s p_a(s)^2 u(s)^2\right) + f\frac{d}{ds}u(s) + \frac{u(s)}{\theta} = 0. \tag{11}$$

The case $s = 1$ must be treated separately. The terms containing $\frac{s}{2}$ or $s-1$ in Eq. (9) vanish, while formation of new clusters comes into play. A new cluster of size 1 is generated whenever a new tree is planted at a site which is neither part of an existing cluster itself nor of its total perimeter.

Neglecting the overlap of the perimeters of clusters, we obtain

$$\begin{aligned}\delta N_f(1) &= \theta\left(1-\sum_{s=1}^{\infty} N(s)\frac{s+p_t(s)}{A}\right)\\ &= \theta\left(1-(1+f)\sum_{s=1}^{\infty} u(s)\right)\\ &= \theta(1-(1+f)\rho),\end{aligned} \tag{12}$$

where

$$\rho = \sum_{s=1}^{\infty} u(s) \tag{13}$$

is the total tree density, i.e., the number of occupied sites per lattice size.

However, Eq. (12) does not regard the contribution of small clusters correctly as their total perimeter is underestimated by Eq. (2), e.g., $p_t(1)=4$ and $p_t(2)=6$ for real clusters, while Eq. (2) predicts $p_t(1)=0.7$ and $p_t(2)=1.4$. For simplicity, we only apply a correction for $s=1$, so that Eq. (12) turns into

$$\delta N_f(1) = \theta(1-(1+f)\rho-(4-f)u(1)). \tag{14}$$

From this we immediately obtain

$$\frac{16}{\sqrt{2}}u(1)^2+\left(8-f+\frac{1}{\theta}\right)u(1)+(1+f)\rho=1, \tag{15}$$

where we have assumed that $p_a(1)=4$, too, although the underestimation of the accessible perimeter by Eq. (4) is rather weak (Fig. 2).

The basic properties of the model can be derived directly from Eq. (11) without regard to Eq. (15). Let us first insert Eq. (4) into Eq. (11) and rearrange the terms in order to determine the dominating contributions:

$$\left(u(s)+\frac{f}{g^2 s^{2h}}\right)\frac{d}{ds}u(s) = -\left(\frac{h+\frac{1}{2}}{s}u(s)+\frac{1}{\theta g^2 s^{2h}}\right)u(s). \tag{16}$$

On both sides, the terms arising from coalescence (first term in Eq. 11) dominate if

$$u(s) \gg \frac{f}{g^2 s^{2h}} \quad \text{and} \quad u(s) \gg \frac{1}{\theta\left(h+\frac{1}{2}\right)g^2 s^{2h-1}}. \tag{17}$$

In this case, Eq. (11) yields

$$s p_a(s)^2 u(s)^2 = \text{const} \tag{18}$$

and thus in combination with Eq. (4)

$$u(s) \propto s^{-(h+\frac{1}{2})}. \tag{19}$$

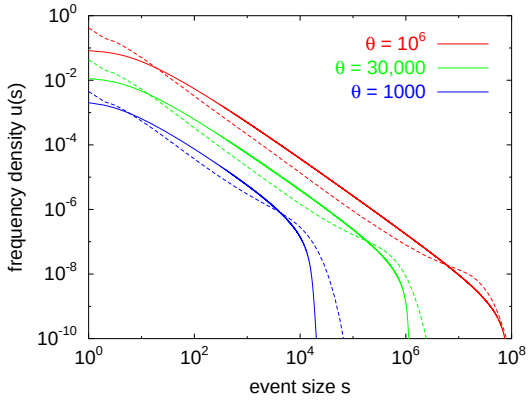

Fig. 3. Event-size distribution in the original DS-FFM (dashed) and in the simplest version of our model (solid) for different growth rates θ. For clarity, the lines with $\theta=1000$ were shifted downwards by one decade, and the lines with $\theta=10^6$ were lifted by one decade.

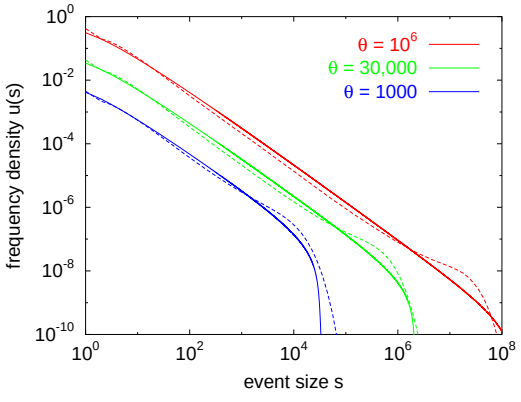

Fig. 4. Event-size distribution of our model using the enforced coalescence according to Eq. (25) (solid) compared to the DS-FFM (dashed). The pairs of lines for $\theta=1000$ and $\theta=10^6$ are shifted as in Fig. 3.

So the frequency density of the fires follows a power law with an exponent

$$\tau = h+\frac{1}{2} = 1.19 \tag{20}$$

in this regime. The scaling exponent τ is solely determined by the scaling exponent of the accessible perimeter, which is a geometric property of the clusters and coincides with that found for percolation clusters. Thus, Eq. (19) relates τ to a property of percolation clusters. We note that the predicted value $\tau=1.19$ matches the value obtained numerically from the data shown in Fig. 1 exactly.

The conditions stated in Eq. (17) define the range of validity of the power-law distribution. Inserting Eq. (19) into the first condition immediately reveals that this condition may be violated at small cluster sizes. This means that coalescence dominates over growth only above a minimum cluster size.

In return, the second condition defines an upper limit where burning starts to disturb coalescence. In both cases, the range strongly depends on the parameter g which quantifies the intensity of coalescence by means of the accessible perimeter.

Quantifying the behavior of $u(s)$ above the upper limit is more difficult. Here we can only state that Eq. (11) yields an exponential decay if coalescence becomes negligible compared to growth and burning:

$$u(s) \sim e^{-\frac{s}{f\theta}}. \tag{21}$$

Figure 3 shows the results obtained by solving Eqs. (11) and (15) numerically. Compared to the DS-FFM (dashed lines), three striking differences occur:

1. The fire size distribution approaches a power law very slowly at small sizes, so that recognizing a power law reliably requires very high growth rates.
2. The characteristic bump in the distribution at the transition from a power law to an exponential decay is not reproduced.
3. The exponential decay is too fast.

With regard to the discussion of Eq. (17), the first observation suggests that coalescence is too weak in our approximation. This may be attributed to the assumption that only clusters of nearly the same size can coalesce. In order to make a quantitative estimate we consider the case that a tree is planted on the accessible perimeter of a given cluster of size s. The mean increase in size due to coalescence with smaller clusters is

$$\delta s = \int_1^s N(\xi)\frac{p_a(\xi)}{A}\xi d\xi = \int_1^s u(\xi)p_a(\xi)d\xi, \tag{22}$$

where we have introduced a continuous size variable for convenience. Based on the power-law behavior of $p_a(s)$ (Eq. 4) and $u(s)$ (Eq. 19) we obtain

$$\delta s = 2u(s)p_a(s)\sqrt{s}\left(\sqrt{s}-1\right) \approx 2u(s)p_a(s)s. \tag{23}$$

Corresponding to our simplification, only clusters with sizes greater than $\frac{s}{2}$ may contribute, which results in

$$\delta\tilde{s} = 2u(s)p_a(s)s\left(1-\sqrt{\frac{1}{2}}\right) \approx 0.3\delta s. \tag{24}$$

Thus, our simplification underestimates coalescence by more than a factor three. In the following, we compensate this by multiplying the coalescence term in Eq. (11) by $\frac{10}{3}$, i. e., replace the term $\frac{1}{2s}$ with $\frac{5}{3s}$:

$$\frac{5}{3s}\frac{d}{ds}\left(sp_a(s)^2u(s)^2\right) + f\frac{d}{ds}u(s) + \frac{u(s)}{\theta} = 0. \tag{25}$$

As shown in Fig. (4), this modification fixes the first problem, but does not change anything at the exponential decay and the transition. In particular, the bump is still not reproduced.

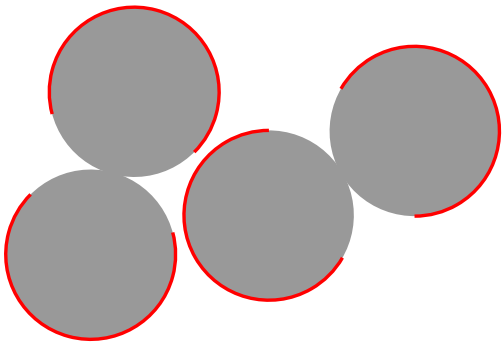

Fig. 5. Schematic illustration of the perimeter available for coalescence with clusters of the same size.

3 The transition to exponential decay

When considering the perimeters of clusters in Fig. 2 we already recognized a deviation of the accessible perimeter from Eq. (4) at large cluster sizes. Above a critical size which depends on θ, the accessible perimeter grows more rapidly with the cluster size than predicted by Eq. (4).

This increase suggests that the shape of the largest clusters differs from that of smaller clusters. The change is related to the result that growth becomes insignificant compared to coalescence for large clusters, leading to a less efficient "smoothing" of the accessible perimeter. As mentioned above (Eq. 18), the coalescence term $sp_a(s)^2u(s)^2$ in Eq. (25) becomes constant, while the growth term is proportional to $u(s)$ and thus decays according to $u(s) \propto s^{-(h+\frac{1}{2})}$. After coalescence of two large clusters, the resulting accessible perimeter should be nearly the sum of the accessible perimeters of the two clusters. Thus coalescence in absence of growth should result in an almost linear increase of the accessible perimeter with the cluster size, similar to the total perimeter, manifested in the deviation from the power law in Fig. 2.

However, this deviation should result in a more rapid decay of $u(s)$ at large sizes in obvious contradiction to the observed bump in the distribution. This is easily recognized since Eq. (18) immediately leads to

$$\frac{d\log u(s)}{d\log s} = -\frac{1}{2} - \frac{d\log p_a(s)}{d\log s}. \tag{26}$$

This relationship generalizes Eq. (19) to the case that the accessible perimeter is not a power-law function and directly relates the slopes $u(s)$ and $p_a(s)$ in double-logarithmic plots. So the decrease of $u(s)$ should simply become steeper at the size s where $p_a(s)$ leaves the power law if the accessible perimeter is responsible for coalescence, provided that coalescence still dominates.

Understanding this phenomenon requires a more thorough consideration of the accessible perimeter that refers to a

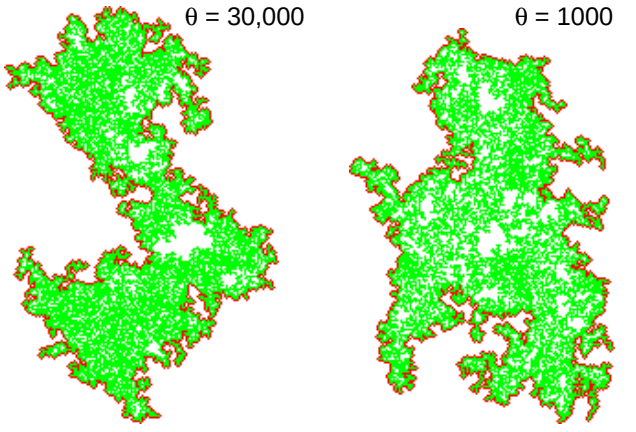

Fig. 6. Two examples of burnt clusters with $s \approx 10\,000$ and $p_a \approx 2000$ at different growth rates $\theta = 30\,000$ and $\theta = 1000$.

small random walker (of size one). Coalescence in absence of growth result in fjord-like perimeter elements which are accessible by a small random walker, but not by another cluster of the same size as required for efficient coalescence. Figure 5 illustrates this effect for two ball-shaped clusters. After coalescence, only two thirds of the resulting perimeter are accessible by identical clusters, leading to $p_a(s) = \frac{4}{3} p_a(\frac{s}{2})$ in this example. This increase is even slower than that predicted by Eq. (4), $p_a(s) = 2^h p_a(\frac{s}{2}) \approx 1.61\, p_a(\frac{s}{2})$. Thus, simple growth is necessary to keep coalescence at its full efficiency.

As an example, Fig. 6 shows two burnt clusters randomly drawn from two simulations with different growth rates. Both are of similar size $s \approx 10\,000$ and accessible perimeter $p_a \approx 2000$, which is close to the value predicted by Eq. (4). While the left one ($\theta = 30\,000$) is in the regime where the power-law distribution perfectly holds, the right one ($\theta = 1000$) is just in the middle of the bump of the distribution (see Fig. 1). Despite their similar sizes and accessible perimeters, significant differences in their shapes are found: The accessible perimeter of the right cluster is less smooth, and there are more large fjord-like structures which are not accessible by a cluster of similar size and shape. Of course, these two clusters are just examples and not completely representative since clusters of the same size strongly vary in shape, but we found at least the same tendency by comparing several clusters.

We describe this effect by introducing a new perimeter $p_c(s)$, the accessible perimeter available for coalescence. According to Eq. (4), p_c should follow the relation $p_c(s) = 2^h p_c(\frac{s}{2})$ as long as growth is strong enough. According to the arguments given above, this may decrease to

$$p_c(s) = \alpha 2^h p_c\left(\frac{s}{2}\right) \tag{27}$$

with $\alpha \approx \frac{2}{3}$ in absence of simple growth. Let us assume that coalescence changes $p_c(s)$ according to Eq. (27), so that an accessible, but non-available part $p_a(s) - p_c(s)$ remains. Trees growing at this non-available part should make this part smaller and the available part larger. As a very simple approach, we assume that each tree growing on the non-available part reduces this part just by one site and increases the available part by one site.

Let us consider a cluster of size s that just originated from two half-sized clusters. In each step it is destroyed by fire or changes its size by further coalescence with the probability

$$\begin{aligned} q &= \frac{s}{A} + \theta\sqrt{\frac{1}{2}} s N(s) \left(\frac{p_c(s)}{A}\right)^2 \\ &= \frac{s + \theta\sqrt{\frac{1}{2}} u(s)\, p_c(s)^2}{A}, \end{aligned} \tag{28}$$

while the probability of a new tree being planted at any perimeter site is $p = \frac{\theta}{A}$. The number of trees n_p planted at each site in the mean before the cluster coalesces again or burns can be computed as follows. In the first step, p trees are planted in the mean. A second step takes place at a probability $1-q$, and the probability that at least k steps are performed is $(1-q)^{k-1}$. As p trees are planted in the mean in each step, we obtain

$$n_p = \sum_{k=1}^{\infty} p(1-q)^{k-1} = \frac{p}{q} = \frac{\theta}{s + \theta\sqrt{\frac{1}{2}} u(s)\, p_c(s)^2}, \tag{29}$$

where the sum was computed using a geometric series. Thus, the probability that a site of the accessible, but not available for coalescence perimeter of a cluster remains in this state is e^{-n_p}, so that this number decays according to

$$p_a(s) - p_c(s) = \left(p_a(s) - \alpha 2^h p_c\left(\frac{s}{2}\right)\right) e^{-n_p}. \tag{30}$$

From this we immediately derive

$$1 - \frac{p_c(s)}{p_a(s)} = \left(1 - \alpha \frac{p_c\left(\frac{s}{2}\right)}{p_a\left(\frac{s}{2}\right)}\right) e^{-n_p}. \tag{31}$$

For solving this equation we assume that the ratio of available and accessible perimeter does not change strongly as s doubles, namely

$$\frac{p_c\left(\frac{s}{2}\right)}{p_a\left(\frac{s}{2}\right)} \approx \frac{p_c(s)}{p_a(s)}. \tag{32}$$

Under this approximation we obtain

$$\frac{p_c(s)}{p_a(s)} = 1 - \frac{1-\alpha}{e^{n_p} - \alpha} \tag{33}$$

Analyzing this equation with n_p from Eq. (29) numerically reveals that the second term in the denominator in Eq. (29) is

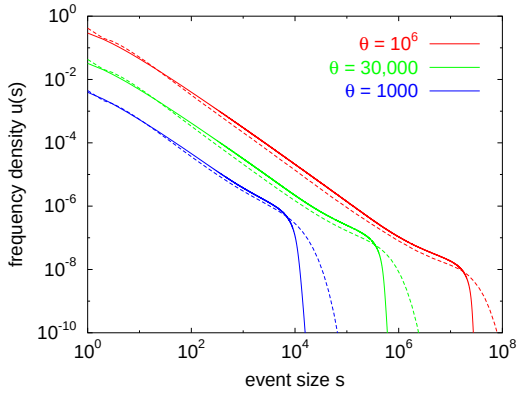

Fig. 7. Event-size distribution of our model using $p_c(s)$ (Eq. 34) instead of $p_a(s)$ (solid) compared to the DS-FFM (dashed). The pairs of lines for $\theta = 1000$ and $\theta = 10^6$ are shifted as in Fig. 3.

negligible, so we can assume $n_p = \frac{\theta}{s}$, and thus

$$p_c(s) = p_a(s)\left(1 - \frac{1-\alpha}{e^{\frac{\theta}{s}} - \alpha}\right). \tag{34}$$

So $p_c(s)$ starts to fall below $p_a(s)$ significantly at $s \approx \theta$.

Figure 7 shows numerical results of our model after replacing the accessible perimeter $p_a(s)$ by $p_c(s)$ in comparison to the original DS-FFM. The power-law regime and the transition to the bump is reproduced perfectly, including the dependence of the transition on θ. Only a vertical shift between the curves remains, but this is not surprising because our assumptions on the perimeters are only valid for large clusters, while both total and accessible perimeters of small clusters are still underestimated.

However, the exponential decay itself is still too fast. Equation (21), confirmed by our numerical results, predicts a decay which is more than ten times faster than in the DS-FFM. The difference even increases slightly with increasing growth rate. So it seems that growth of large clusters is much more efficient in the DS-FFM than predicted by our approach. At this stage, we attribute this phenomenon to the coalescence of large clusters with small clusters which acts like growth.

4 Summary and conclusions

In sum, we have explained several properties of the DS-FFM under quite simple assumptions: Clusters of trees are characterized by their size and their perimeter only, spatial correlations between clusters are neglected, coalescence of clusters is restricted to clusters of similar sizes, and a difference in the shapes of coalescence-generated and growth-generated clusters was introduced.

Beyond these simplifications, the scaling properties of the clusters' total and accessible perimeters were used (Eqs. 2 and 4). These relationships involve 3 nontrivial parameters f, g, and h. The values of these parameters are known for percolation clusters, and we verified numerically that the clusters of the DS-FFM exhibit the same scaling behavior.

Our approach suggests that the power-law regime of the event-size distribution arises from coalescence and derives the scaling exponent $\tau = 1.19$ from the scaling exponent h of the accessible perimeter alone (Eq. 20). As the latter coincides with that of percolation clusters, our approach derives the power-law distribution of the fires in DS-FFM including the scaling exponent from properties of percolation clusters. The other scaling parameters of percolation clusters (f and g) only determine the range of the power-law distribution.

The bump at the transition to the exponential decay can be explained from the shape of large clusters generated by coalescence. Assuming that only a part of the accessible perimeter is available for coalescence and introducing a simple model for the maintenance of this part by growth allows even a quantitative prediction of the transition. Only the exponential decay at large cluster sizes itself is not reproduced well by our approach. So it seems to be the most complicated property of the DS-FFM under quantitative aspects.

Acknowledgements. This work was funded by the Austrian Science Fund (FWF): P19733-N10. The help of two referees in improving the clarity of the paper is greatly appreciated.

Edited by: N. S. Erokhin
Reviewed by: two anonymous referees

References

Bak, P.: How Nature Works – the Science of Self-Organized Criticality, Copernicus, Springer, Berlin, Heidelberg, New York, 1996.

Bak, P., Tang, C., and Wiesenfeld, K.: Self-organized criticality. An explanation of 1/f noise, Phys. Rev. Lett., 59, 381–384, 1987.

Christensen, K., Flyvbjerg, H., and Olami, Z.: Self-organized critical forest-fire model: mean-field theory and simulation results in 1 to 6 dimensions, Phys. Rev. Lett., 71, 2737–2740, doi:10.1103/PhysRevLett.71.2737, 1993.

Clar, S., Drossel, B., and Schwabl, F.: Scaling laws and simulation results for the self-organized critical forest-fire model, Phys. Rev. E., 50, 1009–1018, 1994.

Drossel, B. and Schwabl, F.: Self-organized critical forest-fire model, Phys. Rev. Lett., 69, 1629–1632, 1992.

Gabrielov, A., Newman, W. I., and Turcotte, D. L.: Exactly soluble hierarchical clustering model: Inverse cascades, self-similarity, and scaling, Phys. Rev. E., 60, 5293–5300, doi:10.1103/PhysRevE.60.5293, 1999.

Grassberger, P.: On a self-organized critical forest fire model, J. Phys. A, 26, 2081–2089, 1993.

Grassberger, P.: Critical behaviour of the Drossel-Schwabl forest fire model, New J. Phys., 4, 17.1–17.15, doi:10.1088/1367-2630/4/1/317, 2002.

Grossman, T. and Aharony, A.: Structure and perimeters of percolation clusters, J. Phys. A: Math. Gen., 19, L745–L751, doi:10.1088/0305-4470/19/12/009, 1986.

Henley, C. L.: Statics of a "self-organized" percolation model, Phys. Rev. Lett., 71, 2741–2744, 1993.

Honecker, A. and Peschel, I.: Lenght scales and power laws in the two-dimensional forest-fire model, Physica A, 239, 509–530, 1997.

Jensen, H. J.: Self-Organized Criticality – Emergent Complex Behaviour in Physical and Biological Systems, Cambridge University Press, Cambridge, New York, Melbourne, 1998.

Krenn, R. and Hergarten, S.: Cellular automaton modelling of lightning-induced and man made forest fires, Nat. Hazards Earth Syst. Sci., 9, 1743–1748, doi:10.5194/nhess-9-1743-2009, 2009.

Kunz, H. and Souillard, B.: Essential singularity in percolation problems and asymptotic behavior of cluster size distribution, J. Stat. Phys., 19, 77–106, doi:10.1007/BF01020335, 1978.

Malamud, B. D., Morein, G., and Turcotte, D. L.: Forest fires: an example of self-organized critical behavior, Science, 281, 1840–1842, 1998.

Moßner, W., Drossel, B., and Schwabl, F.: Computer simulations of the forest-fire model, Physica A, 190, 205–217, 1992.

Olami, Z., Feder, H. J. S., and Christensen, K.: Self-organized criticality in a continuous, nonconservative cellular automation modeling earthquakes, Phys. Rev. Lett., 68, 1244–1247, 1992.

Pastor-Satorras, R. and Vespignani, A.: Corrections to scaling in the forest-fire model, Phys. Rev. E., 61, 4854–4859, 2000.

Pruessner, G. and Jensen, H. J.: Broken scaling in the forest-fire model, Phys. Rev. E., 65, 056707, 2002.

Schenk, K., Drossel, B., and Schwabl, F.: Self-organized critical forest-fire model on large scales, Phys. Rev. E., 65, 026135, 2002.

Zinck, R. D. and Grimm, V.: More realistic than anticipated: A classical forest-fire model from statistical physics captures real fire shapes, Open Ecol. J., 1, 8–13, doi:10.2174/1874213000801010008, 2008.